A Dynamic Consensus Algorithm based Low-Voltage Ride-Through Operation of Power Converters in Grid-Interactive Microgrids

Zhao, Xin; Meng, Lexuan; Savaghebi, Mehdi; Quintero, Juan Carlos Vasquez; Guerrero, Josep M.; Wu, Xiaohua

Published in:
Proceedings of IECON 2016: The 42nd Annual Conference of IEEE Industrial Electronics Society

DOI (link to publication from Publisher):
10.1109/IECON.2016.7794078

Publication date:
2016

Document Version
Early version, also known as pre-print

A Dynamic Consensus Algorithm based Low-Voltage Ride-Through Operation of Power Converters in Grid-Interactive Microgrids

Xin Zhao, Lexuan Meng, Mehdi Savaghebi, Juan C. Vasquez, Josep M. Guerrero
Department of Energy Technology
Aalborg University
Aalborg, Denmark
{xzh, lme, mes, juq, joz}@et.aau.dk

Xiaohua Wu
School of Automation
Northwestern Polytechnical University
Xi'an, China
wxh@nwpu.edu.cn

***Abstract*—The possibility of increasing penetration level of grid-interactive microgrids (MGs) has gained a great interest over the past decade. Thus, it is critical to investigate the performance of the MGs under voltage sags, since it may induce instability to the power grid. Negative sequence droop control based voltage support strategy has been proposed to aid MGs riding through three phase asymmetrical voltage sags. However, since the line impedance from each converter to the point of common coupling (PCC) is not identical, both positive sequence and negative sequence output current of the converters cannot be equally shared if no extra current balancing loop is added. Accordingly, a dynamic consensus algorithm (DCA) based negative/positive sequence current sharing scheme is proposed in this paper. Finally, a lab-scale AC microgrid was designed and tested in the lab to validate the feasibility of the proposed control method.**

Keywords—grid-interactive microgrid, low-voltage ride-through, hierarchical control, consensus algorithm.

I. INTRODUCTION

Recently, due to the continuously increasing installation of microgrids (MGs) [1], Denmark and German had revised their grid codes to require distributed generators (DGs) to provide reactive power support and low-voltage ride-through (LVRT) capability [2]-[3]. Unfortunately, the published grid code requirements mainly focus on wind farms linked with medium voltage (MV) or high voltage (HV) grid, while, in a near future, these interconnection standards could be extended to low voltage (LV) grids [4].

Conventionally, LVRT strategy for wind power systems have the objective of nullifying the power oscillations or injecting balanced current into the grid by controlling the grid-interactive converter [5]. Under this condition, the converter normally operates in current-controlled mode. Besides, LVRT of PV converters is also achieved by controlling the grid-interactive converter as a current source which phase angle signal is sensed from the grid voltage to achieve unity power factor current, meanwhile a dedicated current control loop assures the power injection accuracy and harmonic issues [4], [6]. However, to the best of authors knowledge, the exact methodologies on how to achieve LVRT in droop controlled converters are rarely studied [7]. In [6], a droop method based strategy is proposed to embed the PV inverter with both harmonic compensation and voltage support capability, however, the line impedance is considered mainly inductive which limits its application in a real case. A reactive power compensation strategy, which takes the complex line impedance into account, is proposed in [8], however, only single phase application has been discussed. In [9] and [10], a LVRT control scheme, which is based on negative sequence droop strategy, is presented to achieve power injection under asymmetrical voltage sags. The results of [10] show that both the positive and negative sequence current can be equally shared under voltage sags, however, all the distribution line impedance was considered identical in the paper. As a consequence, the injected power may deviate from the reference if the line impedance is asymmetrical. In order to overcome this issue and achieve accurate current sharing during the period of voltage sag, a dynamic consensus algorithm (DCA) [11]-[13] based current sharing strategy is proposed in this paper by adding extra output impedance to the converter to equally share the injected power. With the proposed current sharing strategy, only low bandwidth communication between neighboring units are required to achieve accurate current sharing.

The rest of this paper is organized as follows. Section II presents phasors analysis during voltage sags while Section III illustrates the proposed hierarchical control scheme, including inner voltage/current loops, positive/negative sequence droop control loops and DCA based current sharing loop. Experimental results from two paralleled 2.2 kW converters forming a grid-interactive microgrid are given in Section IV. Finally, the conclusions are illustrated in Section V.

II. POWER FLOW ANALYSIS UNDER VOLTAGE SAGS

According to the symmetrical component theory, the

The work has been supported by the Danish Energy Technology Development and Demonstration Program through the Sino-Danish Project "Microgrid Technology Research and Demonstration" and by the International Science & Technology Cooperation Program of China, Project Number: 2014DFG62610.

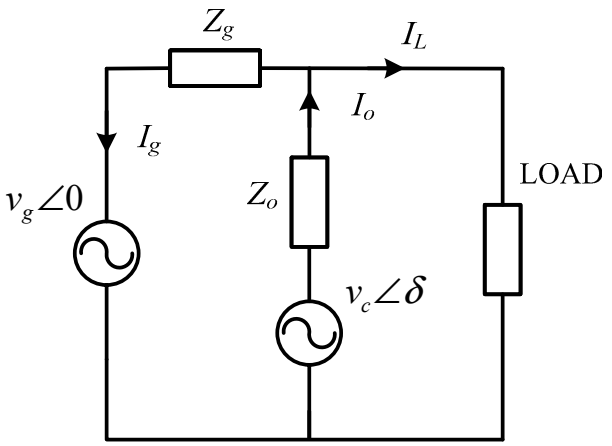

Fig. 1. Power flow analysis.

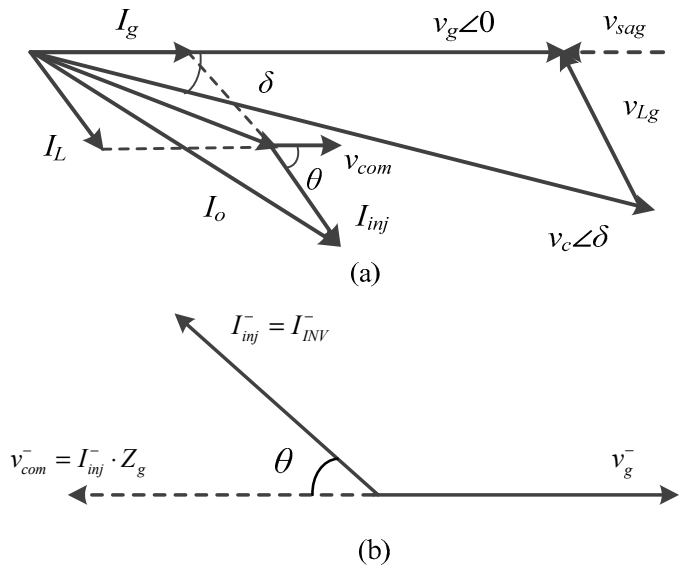

Fig. 2. Phasor diagram of the grid-interactive converter with complex line impedance under voltage sags. (a)positive and (b) negative sequence.

positive and negative sequence components are decoupled from each other. Thus, it is possible to implement different control methods on different sequence components. Thanks to this feature, various control objectives can be achieved, e.g. maximum positive sequence voltage restoration or maximum voltage unbalance mitigation.

Power flow diagram between the grid and the converter is depicted in Fig. 1, where v_c and v_g represent the converter output voltage and grid voltage, respectively. Z_o and Z_g represent the converter closed-loop output impedance, and the grid impedance, respectively. I_o, I_L, and I_g denote the converter current, load current, and grid current, respectively.

Since the MG is usually a LV grid, impedance of the grid can be considered mainly resistive. Also, taking into account the leakage inductance of the transformer, which usually locates at the PCC, both resistance and inductance should be taken into consideration. The positive and negative sequence phasor diagrams are illustrated in Figs. 2(a) and (b). In this figure, θ stands for the angle of Z_g, while v_c and v_g correspond to the converter voltage and grid voltage, respectively. Note that '−' denotes the negative sequence component.

As it can be seen in Figs. 2(a) and (b), due to the complex grid impedance, the inverter should provide both reactive power and active power support to the grid to mitigate the negative sequence voltage as well as restore the positive sequence voltage.

III. Hierarchical LVRT Control Scheme

For the purpose of achieving LVRT and also enhance current sharing accuracy, a hierarchical control algorithm [14]-[15], which consists of two control levels, is proposed in this paper. The overall control schematic diagram is illustrated in Fig. 3.

A. Primary Controller

Primary controller mainly concludes droop control, virtual impedance, and the voltage/current inner controller. The voltage/ current inner controller mainly responsible for voltage/current regulation, while the virtual impedance and the droop control contributes to power sharing accuracy enhancement [13]. Besides, the converter output current and capacitor voltage is measured for active and reactive power calculation. The calculated active power P and reactive power Q are then fed to the droop controller for power sharing and circulating current suppression. The droop law can be defined as follows:

$$\varphi^* = \varphi_0 - \left(m_p + \frac{m_I}{s} \right)\left(P - P_{ref} \right) \tag{1}$$

$$E^* = E_0 - n_p \left(Q - Q_{ref} \right) \tag{2}$$

where E^* and φ^* denote the phase angle and amplitude of the voltage reference while E_0 and φ_0 denote the rated value of the voltage amplitude and phase angle, P_{ref} and Q_{ref} denote the active power and reactive power reference, respectively, m_p, m_I and n_I are the proportional and integral coefficients for the droop controllers, respectively.

In addition, the virtual impedance control is applied, since it can make system more damped and provides better P/Q decoupling with appropriate output impedance shaping [10]. Note that all the primary loop controllers are implemented in $\alpha\beta$ reference frame along with proportional-resonant (PR) controller [11].

B. Secondary Controller

The DCA based LVRT controller mainly responsible for the positive/negative sequence power control and its sharing among the distributed converters. As can be seen in Fig. 3, PCC voltage and current signals are first measured to calculate positive/negative sequence power, and afterwards it is sent to the positive/negative sequence droop controller [10] to generate the positive/negative sequence compensation signal which is connected with the primary controller via a low bandwidth communication link. Finally, the compensation command is added to the primary loop and adjusts the voltage reference in

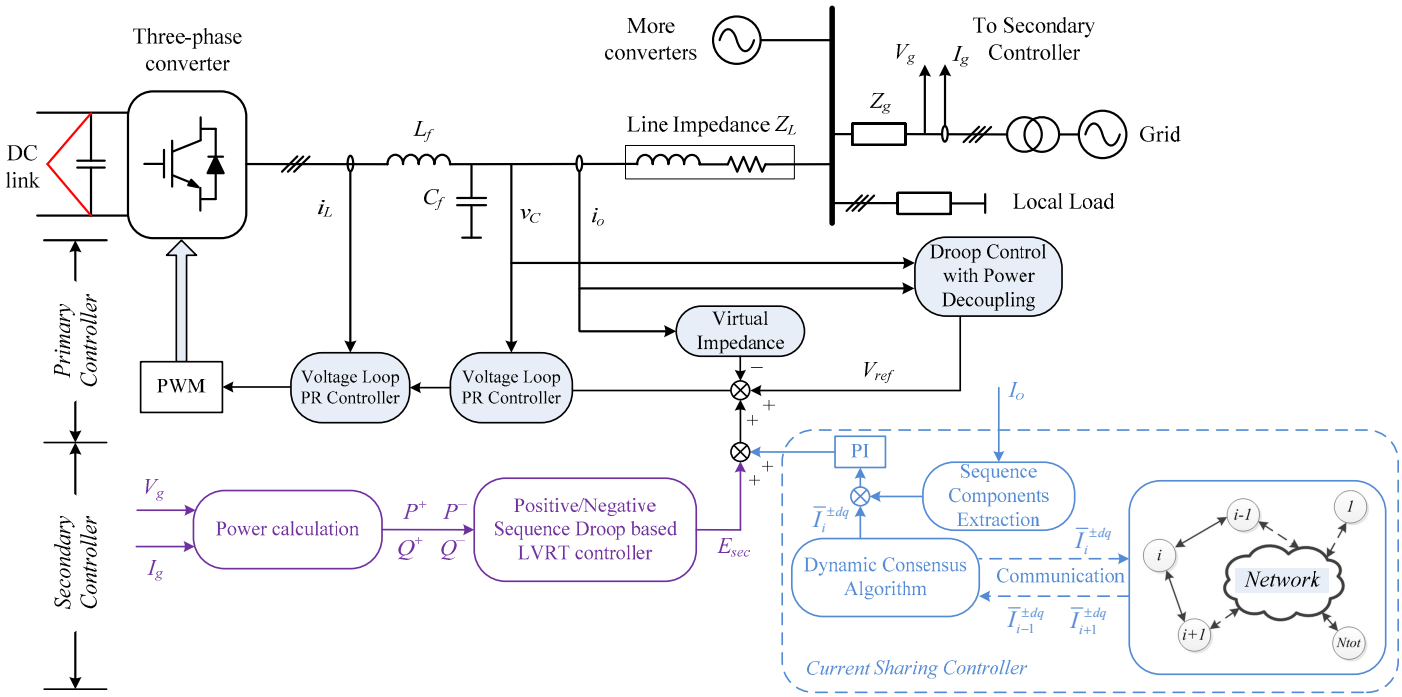

Fig. 3. DCA based hierarchical control scheme.

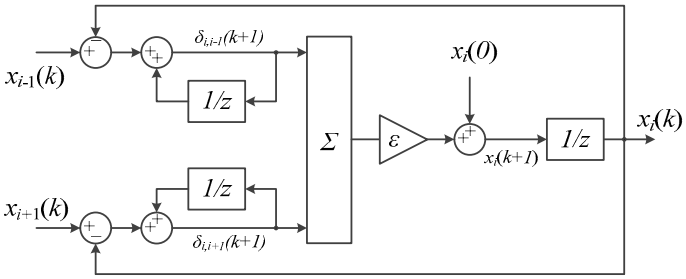

Fig. 4. Block diagram of DCA

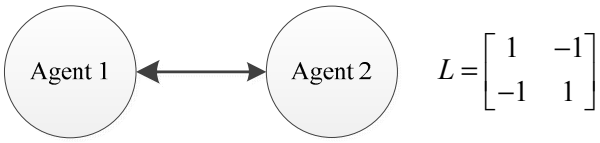

Fig. 5. Adopted communication topology and the corresponding Laplacian matrix

DG side, such that the required amount of power can be injected into the grid.

For the purpose of balancing positive/negative sequence current under asymmetrical line impedance, a current balancing controller is proposed in the secondary control loop. The dq component of the positive/negative sequence converter output current ($I_i^{\pm dq}$) is compared with the average value of the dq components of the positive/negative sequence current ($\bar{I}_i^{\pm dq}$). Then, the resulting signal error is sent to a PI regulator which output command is sent to local controller and added with the converter voltage reference after transform to $\alpha\beta$ reference frame. Note that $\bar{I}_i^{\pm dq}$ is obtained by using DCA which will be illustrated in Section IV.

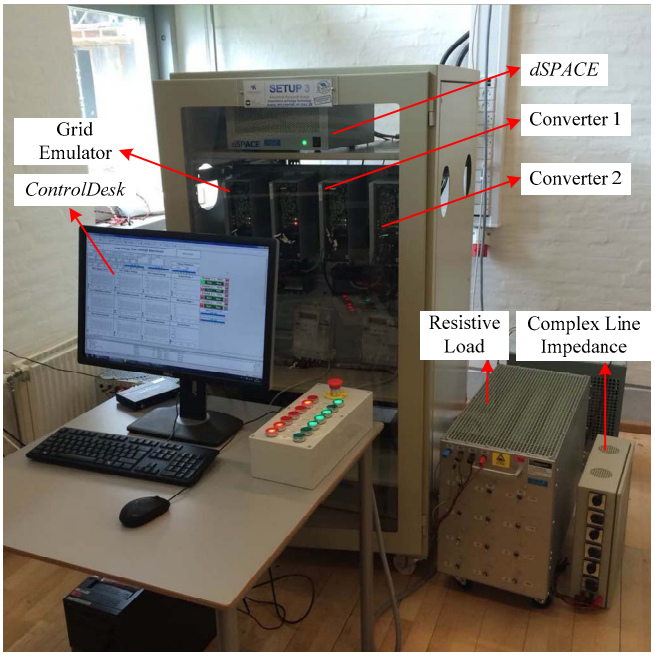

Fig. 6. Experimental testbed.

IV. Consensus Algorithm

Generally, consensus algorithm is applied to obtain a convergence in an environment with dynamically changing variables. In this studied case, DCA [12]-[13], which is an improved consensus algorithm, is used to realize the positive/negative sequence current information sharing and coordination among the distributed converters. Schematic of the DCA is illustrated in Fig. 4, and its mathematical expression is shown as follows.

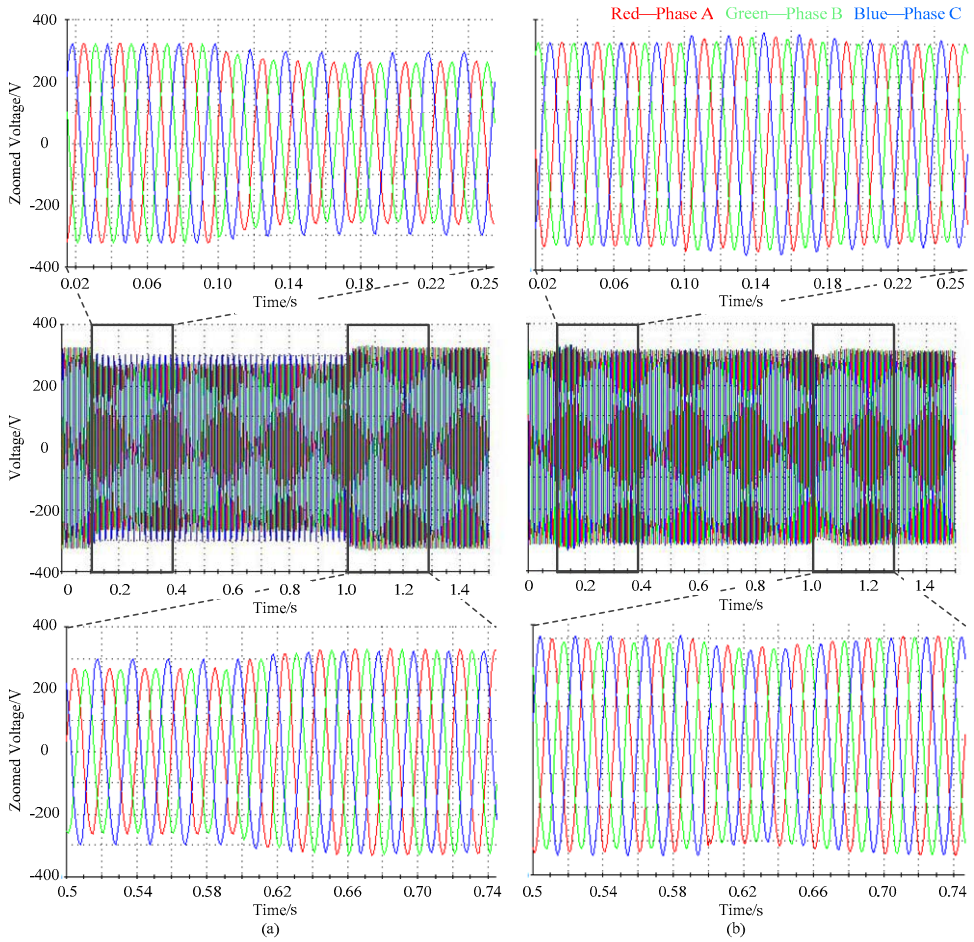

Fig. 7. Voltage waveforms. (a) grid side voltage, and (b) load side voltage.

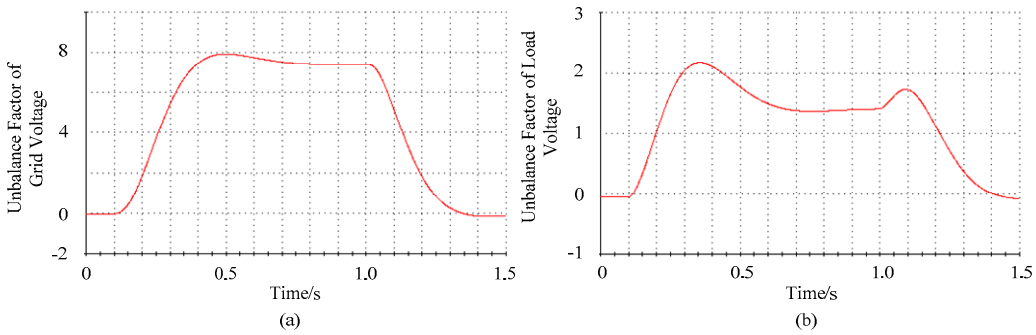

Fig. 8. Unbalance factor waveforms. (a) grid voltage unbalance factor, and (b) load voltage unbalance factor.

$$x_i(k+1) = \varepsilon \cdot \sum_{j \in N_i} \delta_{ij}(k+1) + x_i(0) \tag{3}$$

$$\delta_{ij}(k+1) = a_{ij} \cdot \left(x_j(k) - x_i(k) \right) + \delta_{ij}(k) \tag{4}$$

where ε is the value of constant edge weight between agents. $\delta_{ij}(k)$ is the cumulative error between two agents, and $\delta_{ij}(0)$ equals to 0. Note that $a_{ij} > 0$, only when agent i and agent j are neighbors.

In this paper, $x(k)$ stands for the calculated average value of the positive/negative sequence current, while $x(0)$ stands for the measured positive/negative sequence current. According to all the calculated and measured current information, DCA will aid each converter to calculate the average value of positive/negative sequence current.

Also, the constant edge weight ε, which determines the system dynamics, is defined as follows

$$W = I - \varepsilon \cdot L \tag{5}$$

where L is the Laplacian matrix [11] of the communication topology. The adopted communication topology and the resulting Laplacian matrix is shown in Fig. 5. According to [12], ε can be calculated as (6) to obtain the fastest convergence speed.

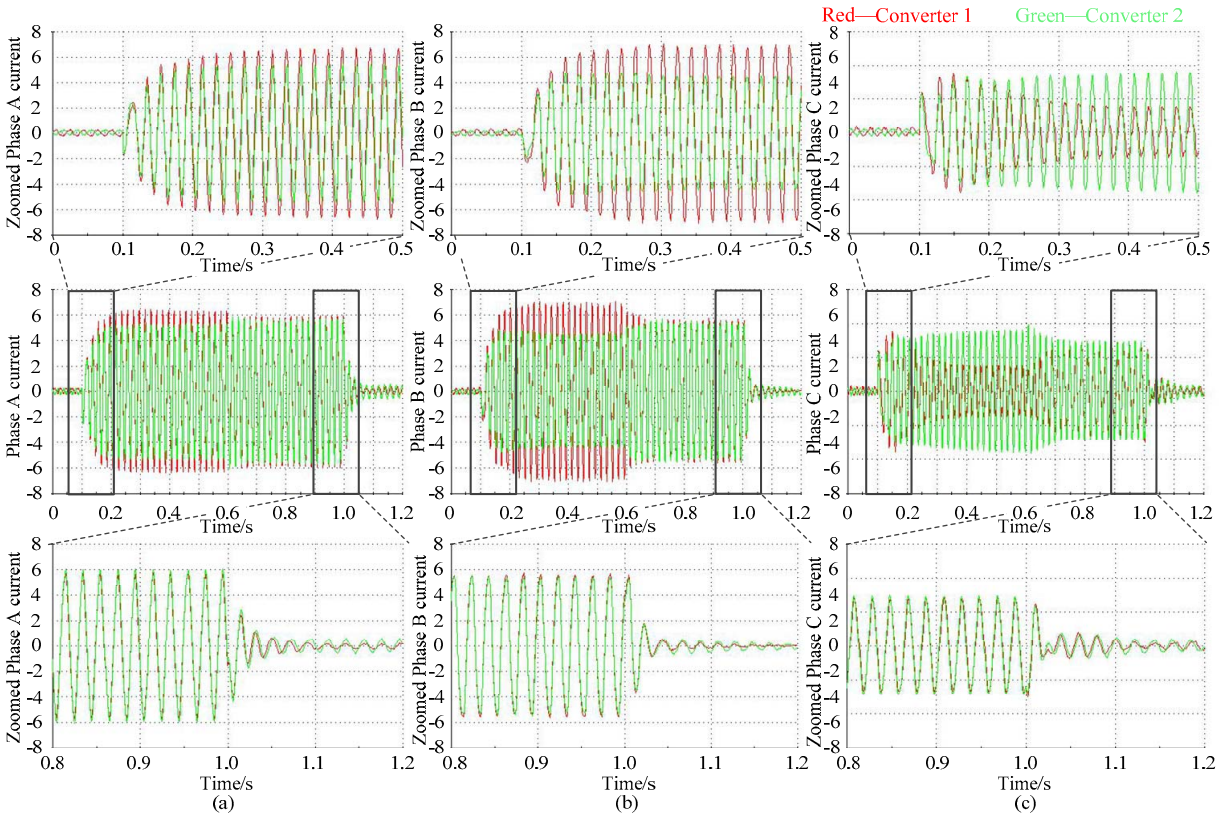

Fig. 9. Output current of the two converters. (a) phase A, (b) phase B, and (c) phase C.

$$\varepsilon = \frac{2}{\lambda_{n-1}(L) + \lambda_1(L)} \tag{6}$$

where λ_n is the n^{th} largest eigenvalue of matrix L. ε is set to 1 in this paper, since a bi-directional communication link is established between two control systems.

V. Experimental Results

To validate the proposed control strategy, experiments are conducted and the results are included below. The whole experimental setup is depicted in Fig. 6, while corresponding power stage schematic can be seen in Fig. 3. Moreover, specifications of the experimental setup are listed in Table I. In experimental testbed, two three-phase converters are connected in parallel with the grid through complex line impedance (Z_g=2 + j2 Ω).

A 0.2 p.u. two phase voltage sag, which occurs at t = 0.1s and clears at t = 1s, is created to test the effectiveness of the DCA based current sharing controller, and the corresponding voltage waveform is depicted in Fig. 7(a).

Fig. 7(b) illustrated load voltage. In contrast with the grid voltage, the load voltage is restored to its nominal value and all three phase voltages becomes balanced as a result of the positive and negative sequence current injection. Moreover, Fig. 8 depicts the load voltage and grid voltage unbalance factor. As shown in the figure, the load voltage unbalance factor decreased significantly thanks to the negative sequence power injection. Consequently, the local electrical load can be protected from potential damages.

TABLE I. System Parameters

Parameters of the Power Stage			
Parameters	***Symbol***	***Value***	***Unit***
Grid Inductance	L_g	*1.8*	*mH*
LCL filter Inductance	L_f	*1.8*	*mH*
Filter Capacitance	C	*9*	*μF*
Nominal Voltage	V	*230*	*V*
Nominal Frequency	f	*50*	*Hz*
DC Voltage	V_{DC}	*650*	*V*
Switching Frequency	f_s	*10*	*kHz*
Line Impedance	Z_{L1}	*1+j1*	Ω
Line Impedance	Z_{L2}	*4+j2*	Ω
Primary Controller			
Parameters	***Symbol***	***Value***	
Voltage Controller	k_{vp}, k_{vr}	*0.05, 30*	
Current Controller	k_{ip}, k_{ir}	*2, 200*	
Proportional Phase Droop	m_P	*0.0005 Rad·s/W*	
Integral Phase Droop	m_I	*0.00006 Rad/W*	
Proportional Voltage Droop	n_P	*0.002 V/Var*	
Integral Voltage Droop	n_I	*0.005 V/Var*	
Virtual Resistor	R_v	*1* Ω	
Virtual Inductor	L_v	*4 mH*	
Secondary Controller			
Parameters	***Symbol***	***Value***	
Proportional Components	k_p	*0.01*	
Integral Components	k_I	*0.02*	
Constant Edge Weight	ε	*1*	

In order to examine the transient response and current sharing accuracy of DCA based LVRT controller, the three phase output currents of the converters are illustrated in Fig. 9.

However, the phase current between the converters cannot be shared equally due to the asymmetrical line impedance. Thus, to equally share the load current between the converters, DCA based current sharing controller is enabled at t = 0.6s (see Fig. 9). As it can be seen, after the current sharing loop is activated, the output current converges to the average value.

VI. Conclusion

This paper proposes a dynamic consensus algorithm based current sharing scheme during voltage sags. The power flow of the overall system is illustrated, the LVRT and DCA based current sharing strategy are also analyzed and discussed. Experimental testbed which contains two converters and the grid are constructed to validate the effectiveness of the proposed control strategy. The experimental results indicate that both the negative and positive sequence power can be injected properly to restore as well as balance the load side voltage. Moreover, thanks to the DCA based current sharing loop, the converter output current is able to converge to the average value accurately even with asymmetrical line impedances.

References

[1] P, Basak, A. Saha, S. Chowdhury, and S. Chowdhury, "Microgrid: Control techniques and modeling," *IEEE Universities Power Engineering Conference*, pp. 1–5, Sep. 2009.

[2] A. Camacho, M. Castilla, J. Miret, R. Guzman, and A. Borrell, "Reactive Power Control for Distributed Generation Power Plants to Comply With Voltage Limits During Grid Faults," IEEE Trans. Power Electron., vol. 29, no. 11, pp. 6224–6234, Nov. 2014.

[3] N. Jelani, M. Molinas, "Asymmetrical Fault Ride Through as Ancillary Service by Constant Power Loads in Grid-Connected Wind Farm," IEEE Trans. Power Electron. vol. 30, no. 3, pp. 1704–1713, March 2015.

[4] Y. Yang, F. Blaabjerg, and Z. Zou, "Benchmarking of Grid Fault Modes in Single-Phase Grid-Connected Photovoltaic Systems," IEEE Trans. Ind. Appl., vol.49, no.5, pp. 2167–2176, Sept.-Oct. 2013.

[5] S. Hu, X. Lin, Y. Kang, and X. Zou, "An Improved Low-Voltage Ride-Through Control Strategy of Doubly Fed Induction Generator During Grid Faults," IEEE Trans. Power Electron., vol. 26, no. 12, pp. 3653–3665, Dec. 2011.

[6] R. Mastromauro, M. Liserre, T. Kerekes, and A. Dell'Aquila, "A Single-Phase Voltage-Controlled Grid-Connected Photovoltaic System With Power Quality Conditioner Functionality," IEEE Trans. Ind. Electron., vol. 56, no. 11, pp. 4436–4444, Nov. 2009.

[7] J. M. Guerrero, J. Matas, L. García de Vicuña, M. Castilla, and J. Miret, "Decentralized control for parallel operation of distributed generation inverters using resistive output impedance," IEEE Trans. Ind. Electron., vol. 54, no. 2, pp. 994–1004, Apr. 2007.

[8] J. C. Vasquez, R. A. Mastromauro, J. M. Guerrero, and M. Liserre, "Voltage Support Provided by a Droop-Controlled Multifunctional Inverter," IEEE Trans. Ind. Electron., vol. 56, no. 11, pp. 4510–4519, Nov. 2009.

[9] X. Zhao, M. Savaghebi, J. M. Guerrero, J. C. Vasquez, K. Sun, X. Wu, G. Chen, and L. Sun, "Negative Sequence Droop Method based Hierarchical Control for Low Voltage Ride-Through in Grid-Interactive Microgrids," IEEE Energy Convers. Cong. and Expo. pp. 6896–6903, 20-24 Sept. 2015.

[10] X. Zhao, J. M. Guerrero, M. Savaghebi, J. C. Vasquez, X. Wu, K. Sun, "Low Voltage Ride-Through Operation of Power Converters in Grid-Interactive Microgrids by Using Negative-Sequence Droop Control," IEEE Trans. Power Electron., vol. PP, no. 99, pp.1-1.

[11] R. Olfati-Saber, J. A. Fax, and R. M. Murray, "Consensus and Cooperation in Networked Multi-Agent Systems," in Proc. IEEE, vol. 95, no. 1, pp. 215–233, Jan. 2007.

[12] L. X. L. Xiao and S. Boyd, "Fast linear iterations for distributed averaging," 42nd IEEE Int. Conf. Decis. Control, vol. 5, 2003.

[13] L. Meng, X. Zhao, F. Tang, M. Savaghebi, T. Dragicevic, J. Vasquez, and J. Guerrero, "Distributed Voltage Unbalance Compensation in Islanded Microgrids by Using Dynamic-Consensus-Algorithm," IEEE Trans. Power Electron., vol. 31, no. 1, pp. 827–838, Jan. 2016.

[14] J. M. Guerrero, J. C. Vasquez, J. Matas, L. G. de Vicuna, and M. Castilla, "Hierarchical control of droop-controlled AC and DC microgrids—A general approach towards standardization," IEEE Trans. Ind. Electron., vol. 58, no. 1, pp. 158–172, Jan. 2011.

[15] J. M. Guerrero, M. Chandorkar, T. L. Lee, and P. C. Loh, "Advanced Control Architectures for Intelligent Microgrids—Part I: Decentralized and Hierarchical Control," IEEE Trans. Ind. Electron., vol. 60, no. 4, pp. 1254-1262, April 2013.